# A Simple and Efficient Method for Simulating the Electronic Absorption Spectra of Criegee Intermediates: Benchmarking on CH<sub>2</sub>OO and CH<sub>3</sub>CHOO

Julia C. McCoy<sup>†</sup>, Barbara Marchetti<sup>†</sup>, Mushir Thodika<sup>‡</sup> and Tolga N. V. Karsili<sup>†</sup>\*

†University of Louisiana at Lafayette, Louisiana, LA 70503, United States of America

‡Temple University, Philadelphia, PA 19122, United States of America

\*Author to whom correspondence be addressed: tolga.karsili@louisiana.edu

#### Abstract

Criegee intermediates (CIs) play a vital role in the atmosphere – known most prominently for enhancing the oxidizing capacity of the troposphere. Knowledge of their electronic absorption spectra is of vital importance for two reasons: (1) to aid experimentalists in detecting CIs and (2) in deciding if their removal is affected by solar photolysis.

In this manuscript we report a simple and efficient method based on the nuclear ensemble method that may be effectively used to compute the electronic absorption spectra of Criegee intermediates without the need for extensive computation of preparing the initial configurations of the starting geometry. We use this method to benchmark several excited-state electronic structure methods and their efficacy in reproducing the electronic absorption spectra of two well-known cases of CI: CH<sub>2</sub>OO and CH<sub>3</sub>CHOO.

The success and computational feasibility of the methodology is crucial for its applicability to CIs of increasing molecular complexity, that have no known experimentally measured electronic absorption spectra – allowing a guide for experimentalists. Application of the methodology to more complex CIs (e.g., those with extended conjugation or those derived from endocyclic alkenes) will also reveal if solar photolysis becomes a competitive removal process when compared to unimolecular decay or bimolecular chemistry.

### Introduction

Alkene ozonolysis is an important removal process of volatile alkenes emitted into the troposphere. The ozonolysis of a given alkene leads to the formation of a carbonyl-oxide containing compound known as the Criegee intermediate (CI). The chemistry of CIs has received significant recent interest since they play a vital role in the atmosphere – known most prominently for enhancing the oxidizing capacity of the troposphere.<sup>1–4</sup>

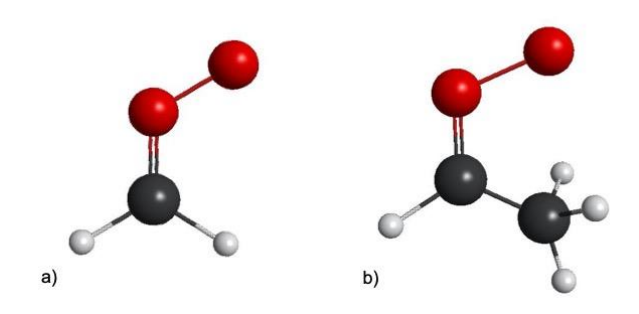


**Figure 1**: Molecular structures associated with (a) formaldehyde oxide and (b) *syn*-acetaldehyde oxide.

The simplest CIs (formaldehyde oxide (CH<sub>2</sub>OO) and acetaldehyde oxide (CH<sub>3</sub>CHOO) – both displayed in fig. 1) have electronic absorption maxima that are well within the tropospherically relevant solar spectrum. Despite the insignificance of solar photolysis for CH<sub>2</sub>OO and CH<sub>3</sub>CHOO in the troposphere,<sup>5,6</sup> understanding the UV absorption profiles of small CIs is none-the-less important as electronic spectroscopy may provide an important probe for the detection of CIs.<sup>7</sup> Additionally, UV-excitation may be a significant contribution to the day-time chemistry of stabilized CIs and suppress the formation of secondary organic aerosols.<sup>8</sup> Despite this, the

photophysics and photochemistry of CIs have received surprisingly little attention when compared to their ground state reactivities. The electronic absorption spectra of the small CIs ( $\leq$ C4) have formed the basis of some experimental<sup>6,9–14</sup> and theoretical<sup>15–18</sup> studies, and it is now understood that the absorption spectra of CIs are dominated by strongly absorbing  $\pi\pi*$  states, local to the carbonyl oxide moiety.<sup>11–13,16,19–22</sup> The spectrum of CH<sub>2</sub>OO and CH<sub>3</sub>CHOO has previously been simulated with elegant techniques that may be difficult to extend to larger CI systems.<sup>15,16,23</sup> Additionally, the majority of studies have used a reduced dimensionality approach for generating the initial starting geometries. Notably, Sršen *et al.*<sup>15</sup> have shown that the computationally demanding high-order CC2/3, ADC(3) and EOM-CCSD/T methods perform well and reproduce the electronic absorption spectra of CH<sub>2</sub>OO and CH<sub>3</sub>CHOO, but these methods are restrictive for larger CIs. Guo *et al.*<sup>16</sup> has also shown that the explicitly correlated variant of multi-reference configuration interaction theory (MRCI-F12) performs exceptionally well when reproducing the electronic absorption spectrum of CH<sub>2</sub>OO, but this method is also difficult to extend to heavier CIs due to its computational demand.

The ensuing dynamics of CIs, following electronic excitation, has also attracted some attention. Using time-of-flight mass spectrometry, Lester and co-workers have demonstrated that UV-irradiation of a CI can lead to quantitative depletion of the CI ion signal (a proxy for the concentration of neutral CIs). 19,20,22 Velocity-Map Imaging studies have shown that this depletion of the ion signal is attributed to UV-induced O-O bond fission, which generates carbonyl-containing molecular products plus oxygen. 24–26 Theoretical photodissociation studies of the simplest CI CH2OO suggest that UV-induced O-O bond cleavage occurs on a picosecond timescale. 16,21,27

Upon increases in molecular complexity, unique differences are observed. For example, a simple extension from CH<sub>2</sub>OO to CH<sub>3</sub>CHOO leads to syn- and anti- conformers, each of which contain markedly (and surprisingly) different electronic absorption maxima. 28 As a result, understanding the electronic absorption spectra of more complex CIs is paramount, primarily because their UV absorption relatively insensitive to variations sections are complexity. 19,20,22,23,29-31 In contrast, loss via bimolecular reaction with water and water dimer strongly depends on the molecular structure (substituents and conformations) of the given CI and their isomeric forms.<sup>31</sup> This suggests that solar photolysis may become highly competitive for certain CI geometries and alkyl chain lengths that disfavor bimolecular reaction. Increasing molecular complexity of CIs could have a profound impact on the relative importance of their atmospheric photochemistries, as bimolecular reactions become less competitive<sup>32</sup> and when a greater number of conformers contribute and introduce a greater selection of unimolecular decay paths. 12,13,23,33,34 Furthermore, additional functional groups may introduce new excited state decay paths that become competitive with O-O bond fission, completely altering the photochemistry and photophysics of the CI. For example, recent experimental studies have focused on the UV-induced photophysics of MVK-OO<sup>35</sup> and methacrolein oxide (MACR-OO)<sup>36</sup>, both of which derive from the ozonolysis of isoprene. In both cases, their absorption spectrum extends into the visible region. This implies that photoexcitation may become a significant tropospheric loss process in MVK-OO and MACR-OO (cf. unimolecular ground state decay). As with CH2OO these experiments on MVK-OO and MACR-OO reveal O-O bond fission but are blind to rival excited state decay paths that may compete with such O-O bond fissions.

In extending to CIs of greater molecular complexity it is important to first understand the simplest cases, CH<sub>2</sub>OO and CH<sub>3</sub>CHOO. Developing an effective yet computationally inexpensive method

that performs well for these small cases is paramount for describing and extending to heavier CIs. Therefore such a method will first need to be tested on the simplest CIs with experimentally known electronic absorption spectra.

In this manuscript we present a simple, yet effective method for computing the electronic absorption spectra of CIs – namely CH<sub>2</sub>OO and CH<sub>3</sub>CHOO – without the need for extensive computation of preparing the initial configurations of the starting geometry. The initial geometries that define the absorption profile are also generated with low computational expense and in a full-dimensional manner – wherein all degrees of freedom of the molecule are considered. Both CH<sub>2</sub>OO and CH<sub>3</sub>CHOO have experimentally measured electronic absorption spectra and thus provide for an effective benchmark. The method, more commonly referred to as the nuclear ensemble method, <sup>37</sup> generates the initial geometries in an even-handed way, and at each returned geometry, computes the vertical excitation energies and transition intensities using high-level multi-reference (or single-reference) methods. Multi- and single- reference methods for computing these vertical excitation energies and therefore simulating the absorption profiles will be benchmarked, in order to ascertain the best computational method for the future computation of the electronic absorption spectra of CIs of greater molecular complexity and with experimentally unknown spectra. The overarching aim is to devise a simple yet versatile technique for computing the absorption spectra that may be used to calculate the UV absorption spectra of CIs of varying molecular complexity. The nuclear ensemble method has previous been successfully applied to simulating the electronic absorption spectra of other atmospherically relevant systems.<sup>38–44</sup>

## **Theoretical Methodology**

The ground state minimum energy geometry of CH<sub>2</sub>OO and CH<sub>3</sub>CHOO was optimized using Grimme's B2PLYP-D3<sup>45</sup> functional of Density Functional Theory, alongside Dunning's correlation-consistent basis set of triple-ζ quality: cc-pVTZ.<sup>46</sup> Normal mode wavenumbers were then computed on the optimized ground state geometry using the same level-of-theory. B2PLYP-D3 has been previously shown to perform well when obtaining the ground state geometry and normal modes of Criegee intermediates.<sup>47,48</sup>

The phase-space of the ground state vibrational level, with n atoms, was modelled using the Wigner distribution<sup>37,49,50</sup> as given in equation 1.

$$P_{W}(\mathbf{q}, \mathbf{P_{q}}) = \frac{1}{(\pi \hbar)^{3n-6}} \prod_{i=1}^{3n-6} exp\left(\frac{-q_{i}^{2}}{2\sigma_{qi}^{2}}\right) exp\left(\frac{-p_{i}^{2}}{2\sigma_{pi}^{2}}\right)$$
(1)

where

$$\sigma_{qi}^2 = \frac{\hbar}{2\mu_i \omega_i} \tag{2}$$

and

$$\sigma_{pi}^2 = \frac{\mu_i \omega_i}{2} \tag{3}$$

In equations 1-3,  $q_i$  is the projected coordinate and  $p_i$  is the associated momentum for each normal mode i with reduced mass  $\mu_i$  and angular frequency  $\omega_i$ . At each returned Wigner geometry, vertical excitation energies and transition dipole moments  $(\vec{\mu}_{ij})$  were computed using a variety of electronic structure methods as described below. The excitation energy dependent photoabsorption cross section P(E) was then obtained using equation 4,

$$P(E) = \frac{\pi e^2}{2m_e c \varepsilon_0} \sum_{j=1}^{M} \left[ \frac{1}{N_{TOT}} \sum_{N=1}^{N_{TOT}} f_{ij}^N g(E - \Delta E_{ij}^N, \delta) \right]$$
(4)

where g is a Lorentzian line shape function given by equation 5,

$$g(E - \Delta E_{ij}^{N}, \delta) = \frac{\hbar \delta}{2\pi} \left( \left( E - \Delta E_{ij}^{N} \right)^{2} + \left( \frac{\delta}{2} \right)^{2} \right)^{-1}.$$
 (5)

 $f_{ij}$  is the oscillator stretch given by equation 6.

$$f_{ij}^{N} = \frac{2}{3} \left( \Delta E_{ij}^{N} \right) \sum_{\alpha = x, y, z} \left| \mu_{ij}^{N} \right|_{\alpha}^{2} \tag{6}$$

and  $\Delta E_{ij}^N = (E_j^N - E_i^N)$ ,  $m_e$  and e are the mass and charge of the electron, respectively, while c is the speed of light. The internal sum in equation 4 is expressed over the set of total Wigner geometries ( $N_{\text{TOT}} = 500$ ) while the external sum includes transitions from the initial state i (the ground state) to final state j (i.e.  $S_1, S_2, S_3, \ldots, S_7$ ) with respective oscillator strengths  $f_{ij}^N$  as given by equation 6.  $\delta$  is a broadening factor, which is arbitrarily set to 0.1 eV for each of the calculated absorption profiles reported herein.

A subset of electronic structure methods was used to calculate the  $E_{ij}^N$  and  $f_{ij}^N$  values in constructing the absorption profiles in equation 4. The methods used were complete active space self-consistent field (CASSCF), complete active space second-order perturbation theory (CASPT2), $^{51-53}$  its explicitly correlated variant (CASPT2-F12), $^{54}$  multi-reference configuration interaction (MRCI) $^{55,56}$  and time-dependent density functional theory (TDDFT). For both CH<sub>2</sub>OO and CH<sub>3</sub>CHOO, the CASSCF computations were state-averaged across seven singlet electronic state configurations. An active space of ten electrons in eight orbitals and twelve electrons in ten orbitals was used. The CASPT2 and MRCI computations were based on a SA7-

CASSCF reference wavefunction, the former method requiring an imaginary level shift of 0.3 *E*<sub>H</sub> in order to mitigate the involvement of intruder states. The TDDFT computations used the ωB97XD<sup>57</sup> and CAM-B3LYP<sup>58</sup> functionals in order to describe both local and long-range correlation effects that may become important. In all cases the aug-cc-pVDZ Dunning basis set<sup>46</sup> was used for the CASSCF/CASPT2(-F12)/MRCI computations whilst 6-311+G(d,p)<sup>59,60</sup> was used for the TDDFT computations. The above-described method is known as the nuclear ensemble method.

The Wigner points were generated using a Newton-X<sup>49,61</sup> subprogram interface, the (TD)DFT used the Gaussian 16 computational package<sup>62</sup> while the CASSCF, CASPT2 and MRCI computations were performed using the Molpro computation package.<sup>63,64</sup>

### **Results and Discussion**

Benchmarking the Electronic Absorption Spectrum of CH<sub>2</sub>OO

Figs. 2 and 3 present the simulated electronic absorption spectra of CH<sub>2</sub>OO calculated using multi-reference and single-reference methodology, respectively. For comparative purposes, the experimentally measured UV absorption spectra, reproduced from Sheps *et al.*, <sup>14</sup> Ting *et al.* <sup>5</sup> and Beames *et al.*, <sup>22</sup> are superimposed on each simulated absorption spectrum. Alongside this figure, table 1 presents the absolute photoabsorption cross sections at the peak maxima of the stimulated absorption spectra at the various levels-of-theory.

**Table 1**: Photoabsorption cross sections (× 10<sup>-17</sup> cm<sup>2</sup>) of CH<sub>2</sub>OO and CH<sub>3</sub>CHOO simulated at the various levels-of-theory.

Method	CH <sub>2</sub> OO	CH <sub>3</sub> CHOO	
		syn-CH <sub>3</sub> CHOO	Anti-CH <sub>3</sub> CHOO
CASPT2(12,10)	1.10	0.81	1.15
CASPT2(10,8)	1.12	0.69	1.05
CASPT2-F12(10,8)	1.02	0.68	1.75
MRCI(10,8)	1.36	0.79	1.20
CAM-B3LYP	2.95	1.81	2.10
wB97XD	2.96	1.78	2.11
	1.23 (ref. <sup>5</sup> )	1.27 (ref. <sup>6</sup> )*	
Experimental	5.00 (ref. <sup>22</sup> )	5.00 (ref. <sup>20</sup> )*	1.20 (ref. <sup>13</sup> )#
	3.60 (ref. <sup>14</sup> )	1.20 (ref. <sup>13</sup> )#	

<sup>\*</sup>Estimated, not directly measured.

We start by considering the electronic absorption spectra that were simulated using the various multi-reference methods, which are displayed in fig. 2. The overlaid experimental spectrum of CH<sub>2</sub>OO, recorded by Ting *et al.* and Sheps *et al.* (panels (a) and (b), respectively), shows a long-wavelength rising-edge at ca. 450 nm which reaches a maximum in absorbance at ca. 350 nm. At hypsochromic wavelengths the absorption cross section drops sharply, with almost no absorption at wavelengths < 300 nm. In contrast the spectrum recorded by Beames *et al.* shows a narrower wavelength distribution. This can be plausibly understood by considering that the electronic absorption spectrum recorded by Beames *et al.* was done so under jet-cooled conditions. As table 1 shows, the experimentally derived photoabsorption cross sections at the peak maxima are mutually inconsistent reinforcing our choice to display normalized intensities rather than absolute photoabsorption cross sections, as returned by equation 5. The photoabsorption cross sections displayed in table 1, for CH<sub>2</sub>OO, agree well with those reported by Sršen *et al.*<sup>15</sup>

<sup>\*</sup>Spectra represents a convolution of both conformers.

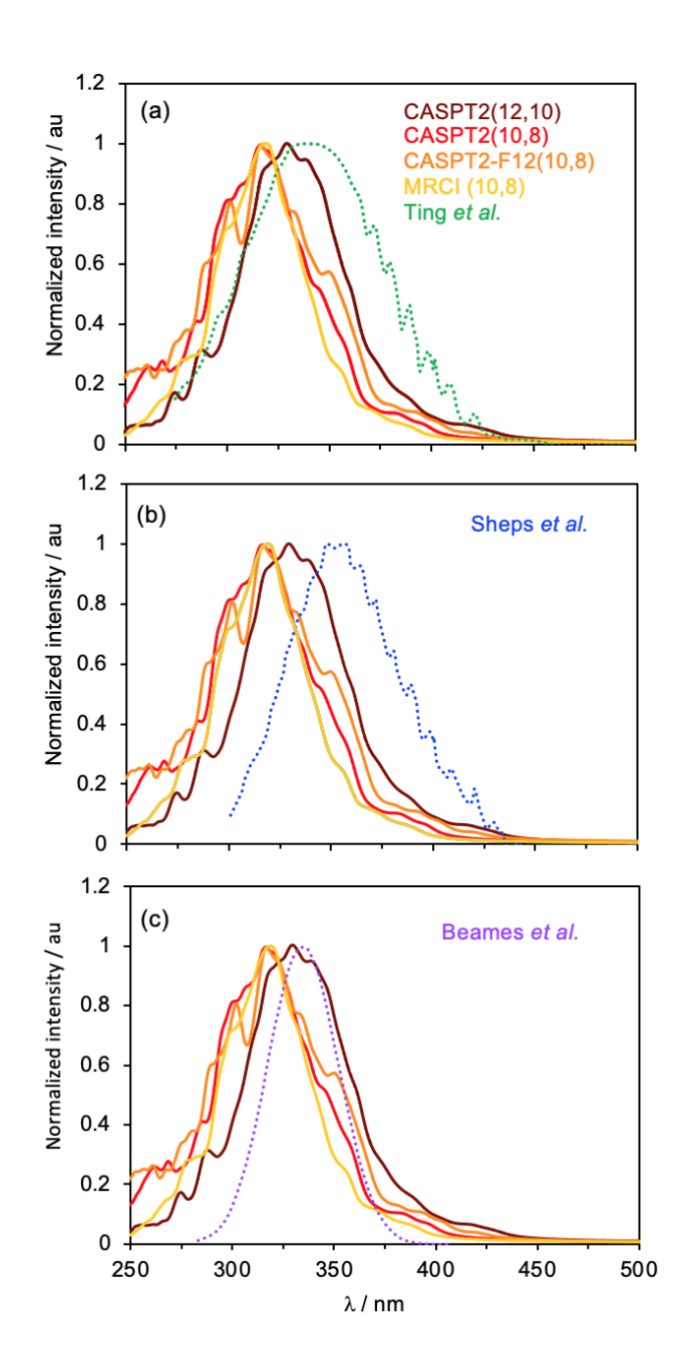


**Fig. 2**: Simulated electronic absorption spectra of CH<sub>2</sub>OO using the multi-reference methods CASSCF, CASPT2, CASPT2-F12 and MRCI. The experimental spectra of (a) Ting *et al.*, (b) Sheps *et al.* and (c) Beames *et al.* are superimposed.

The simulated spectra at the different levels of multi-reference theory are strikingly different. The spectral profiles show that MRCI (based on a SA-CASSCF(10/8) reference) overestimates the excitation energy when compared to CASPT2; the CASPT2 methods are shown to perform moderately better than MRCI, despite the lower computational expense. The spectral profiles computed with CASPT2(10/8) and its explicitly correlated analogue CASPT2-F12(10/8) are almost indistinguishable. Upon increasing the active space to 12 electrons in 10 orbitals (12/10), the spectrum computed at CASPT2(12/10) shows a bathochromic shift (cf. CASPT2(-F12)(10/8) and MRCI). The CASPT2(12/10) profile is in good agreement with the experimental UVabsorption profile measured by Ting et al. (see fig. 2(b)) and in excellent agreement with the UV-absorption profile measured by Beames et al. In the latter case, the better agreement may be a manifestation of the jet-cooled nature of the spectrum recorded by Beames et al. and that a Wigner distribution most closely resembles sampling across the lowest vibrational level of the ground state molecule in a multi-dimensional manner. As noted previously, <sup>16,22</sup> the peak of the absorption band is dominated by a strong  $\pi\pi^*$  excitation – which, as evident from the orbital promotions presented in Figure S3, involves an  $\pi^* \leftarrow \pi$  electron promotion from a wherein the participating orbitals are both localized on the COO moiety.

The spectra computed with CASPT2(12/10) most closely resemble the previously simulated spectra of Guo *et al.*<sup>16</sup>, Sršen *et al.*<sup>15</sup> and Yin *et al.*<sup>23</sup>, which have all used sophisticated, but computationally demanding methods for computing the electronic absorption spectrum of CH<sub>2</sub>OO that require expert experience and knowledge. Additionally, Sršen *et al.* have shown that the most effective methods for simulating the electronic absorption profiles of CH<sub>2</sub>OO and CH<sub>3</sub>-CHOO are the computationally demanding CC3 and ADC(3) methods.

Our present findings on CH<sub>2</sub>OO show that our simple and versatile approach may be used with reasonable computational expense and that the Wigner distribution provides an effective way for generating the ground state ensemble. Additionally, the spectrum obtained with CASPT2 is of comparable quality to the MRCI-F12 absorption profile computed by Guo *et al.* but at a much smaller computational expense. This is a significant benefit of the present methodology for computing the absorption profile, since the much lower computational expense of CASPT2, with a modest active space, may feasibly be used to compute the required 500 Wigner points that make up the spectrum. The methodology may then be feasibly extended to CIs of increasing molecular complexity.

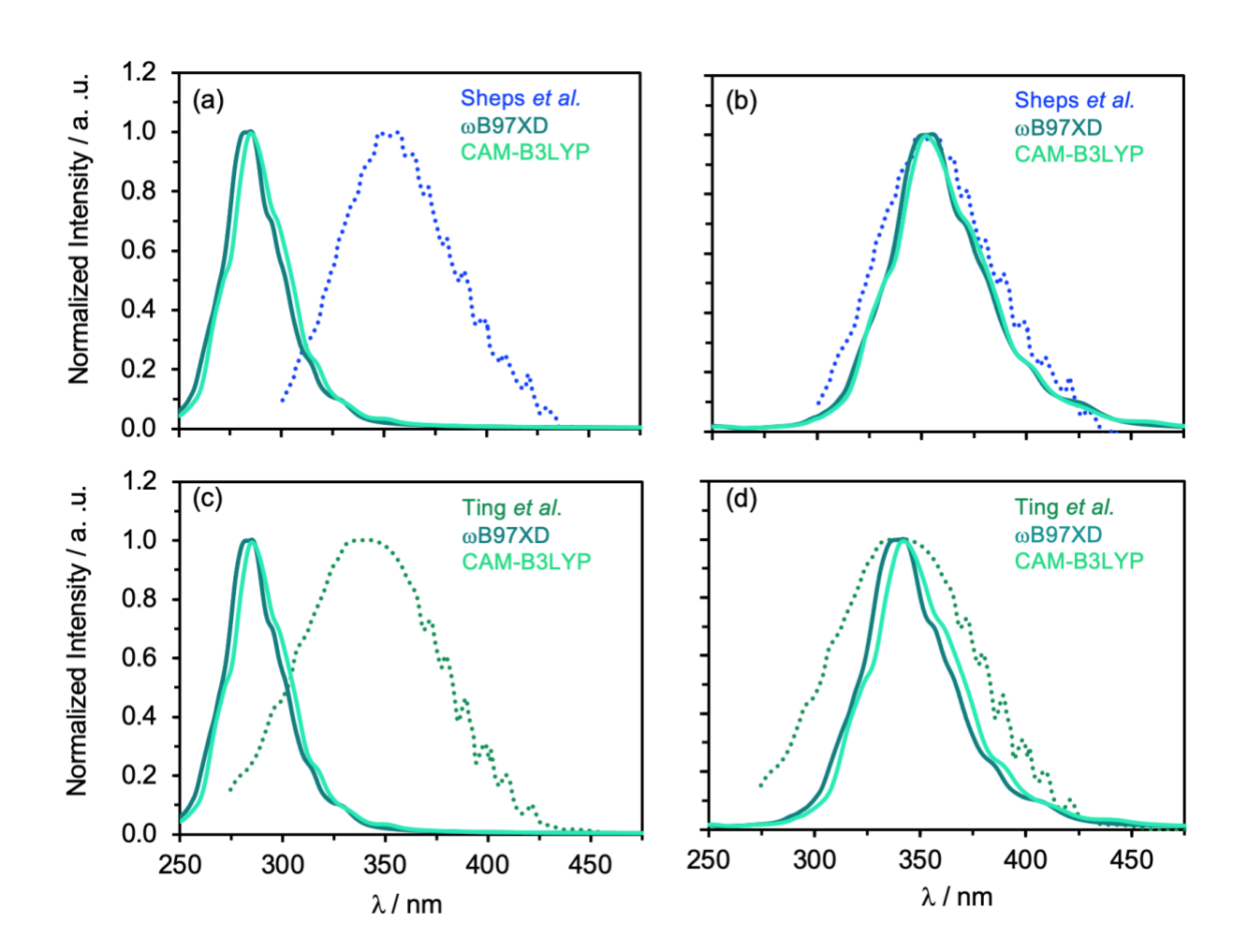


**Fig. 3**: Simulated electronic absorption spectra of CH<sub>2</sub>OO using the single-reference TDDFT functional wB97XD and CAM-B3LYP. Panel (a) shows the ωB97XD and CAM-B3LYP raw simulated alongside the measured electronic absorption spectra by Sheps et al., <sup>14</sup> whilst panel (b) shows the simulated electronic absorption spectrum, shifted in order to match the maximum associated with the experimental spectrum recorded by by Sheps et al. Panels (c) and (d) are analogous to (a) and (b) but are compared and shifted with respect to the measured electronic absorption spectra by Ting et al.<sup>5</sup>

We now turn our attention to the electronic absorption spectra computed using TDDFT. Fig. 3 presents the returned CAM-B3LYP and ωB97XD profiles, presented alongside the experimental UV absorption spectra of CH<sub>2</sub>OO. Panels (a) and (c) feature the same CAM-B3LYP and ωB97XD functionals but are distinguishable by the experimental spectrum to which the simulated spectra are compared. Panel (a) depicts the spectrum recorded by Sheps et al. whilst the panel (c) is that recorded by Ting et al. As evident from figs. 3(a) and 3(c), both DFT functionals overestimate the absorption maximum by ca. 60 nm. This is a common occurrence for vertical excitation energies derived by long-range corrected TDDFT. Despite this, B3LYP and PBE were also benchmarked (see fig. S2 of the supporting information) and both also overestimate the absorption profiles when compared to that measured experimentally. Panels (b) and (d) in fig. 3 show the TDDFT simulated electronic absorption profiles shifted to match the absorption maximum of the measured spectrum recorded by Ting et al. and Sheps et al., respectively. The applied shift in each case is 0.69 and 0.83 eV (to match Ting et al. and Sheps et al., respectively) for the CAM-B3LYP spectra and 0.73 and 0.86 eV (again, to match Ting et al. and Sheps et al., respectively) for the ωB97XD spectra. These same shift values will

be used in the next section to shift the TDDFT profiles of CH<sub>3</sub>CHOO in order to ascertain the extent to which the shift values derived from the simplest CI extend to a more complex CI.

# Benchmarking the Electronic Absorption Spectrum of CH<sub>3</sub>CHOO

Upon ozonolysis of propene, CH<sub>3</sub>CHOO is formed following unimolecular decay of the nascent primary ozonide. CH<sub>3</sub>CHOO represents the simplest alkyl-substituted CI. The addition of a methyl substituent leads to *syn-* and *anti-* conformers of CH<sub>3</sub>CHOO – distinguishable by whether the terminal oxygen atom is pointing towards or away from the CH<sub>3</sub> group, respectively. Both conformers are illustrated in fig. 4.

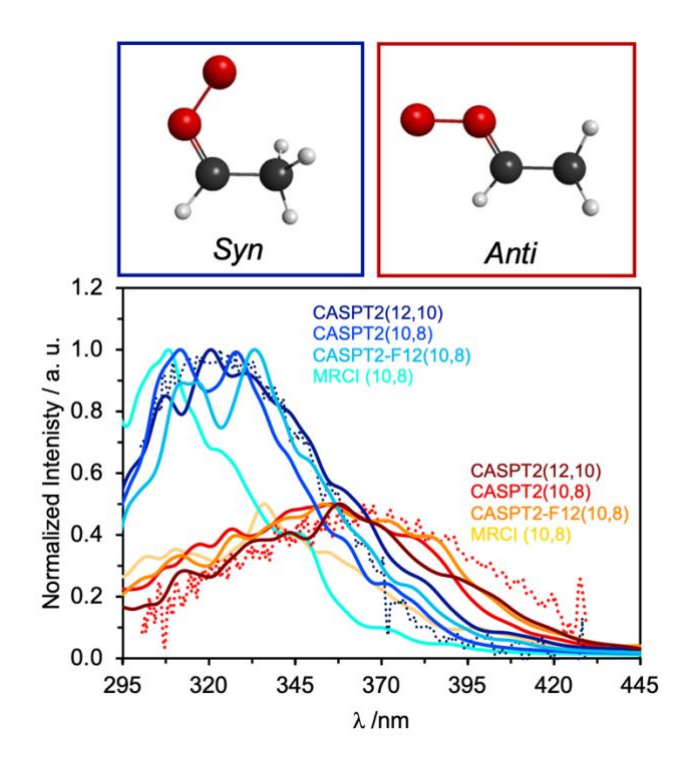


**Fig 4.** Simulated electronic absorption spectra of *syn*- and *anti*- CH<sub>3</sub>CHOO using multi-reference electronic structure methods. Displayed alongside are the measured electronic absorption spectra by Sheps *et al.*<sup>13</sup> (dotted lines).

Fig. 4 presents the experimentally measured and computationally simulated electronic absorption spectra of the syn- and anti- conformers of CH<sub>3</sub>CHOO. In both cases, and as with CH<sub>2</sub>OO, CASPT2 performs far better than MRCI. As with CH2OO, CASPT2 and CASPT2-F12 are of equal quality but the former is less computationally demanding. As evident from fig. 4, the simulated CASPT2 electronic absorption spectra of syn-CH<sub>3</sub>CHOO and anti-CH<sub>3</sub>CHOO are in excellent agreement with the experimentally measured spectra by Sheps et al. 13 and are less sensitive to the active space than those used for the spectral profiles of CH<sub>2</sub>OO. As with CH<sub>2</sub>OO, CASPT2(12,10) may be effectively used to simulate the electronic absorption profile of CH<sub>3</sub>CHOO at a reasonable computational expense. Table 1 presents the absolute photoabsorption cross sections at the peak maxima of the simulated absorption spectra, as returned from equation 5. Since the experimentally derived photoabsorption cross sections of the individual conformers are not directly measured, we cannot directly compare our current results to the experimental spectra. The photoabsorption cross sections displayed in table 1, for CH<sub>3</sub>CHOO, are consistently smaller than those reported by Sršen et al. 15 using the ADC(3) and CC3 methods. Of particular noteworthiness is that both our study and Sršen et al. 15 predict a more intense A-band excitation for anti-CH<sub>3</sub>CHOO (cf. syn-CH<sub>3</sub>CHOO).

We will now discuss the simulated electronic absorption spectra of CH<sub>3</sub>CHOO computed at the TDDFT level – using the CAM-B3LYP and ωB97XD functionals. Fig. 5 presents the simulated electronic absorption profiles of the *syn*- and *anti*- CH<sub>3</sub>CHOO. These simulated spectra are

derived by first computing the absorption profile with the relevant TDDFT functional and then shifting the resulting spectra by the appropriate shift factor derived for CH<sub>2</sub>OO above. The raw unshifted spectra are given in fig. S1 of the supporting information. As evident from fig. 5, following the application of the shift values derived for CH<sub>2</sub>OO, the simulated spectra of CH<sub>3</sub>CHOO accord well with the experimentally measured electronic absorption spectra of both *syn-* and *anti-* CH<sub>3</sub>CHOO. The shifted spectrum derived from Ting *et al.* agree better with the experimental spectral profile of CH<sub>2</sub>OO, when compared to the shift value derived from that of Sheps *et al.* The electronic absorption profiles computed with the CAM-B3LYP and ωB97XD functions are almost indistinguishable owing to the similarity in the parameterization of the longrange components of these functionals. Both functionals also perform well when considering the breadth of the electronic absorption profiles.

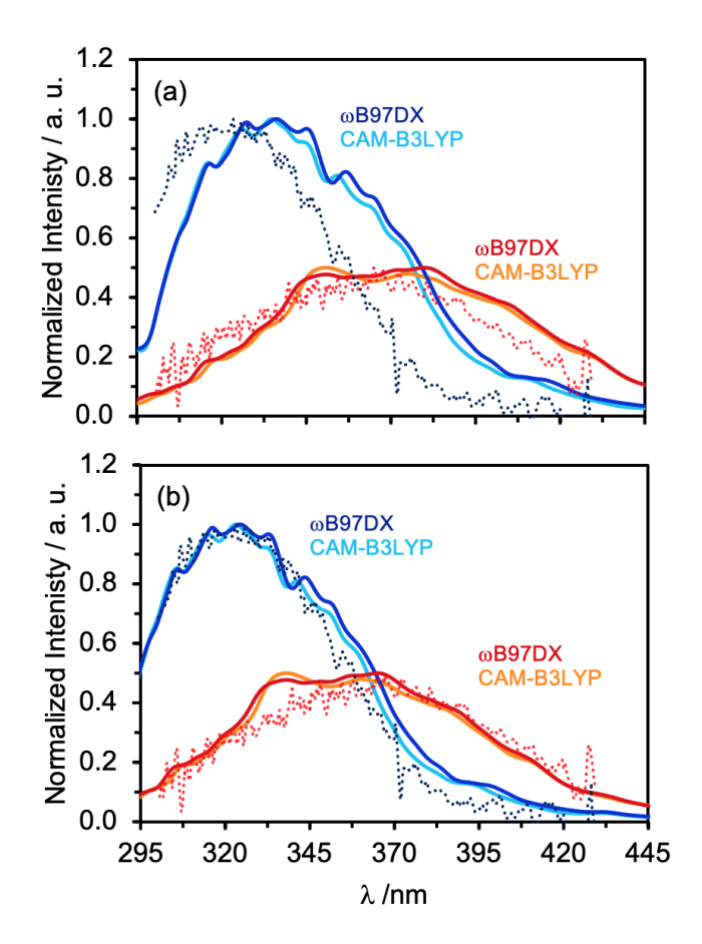


**Fig 5.** Simulated electronic absorption spectra of *syn*- and *anti*- CH<sub>3</sub>CHOO using TDDFT electronic structure methods. Panels (a) and (b) show the shifted TDDFT spectra for *syn*- and *anti*-CH<sub>3</sub>CHOO, using the bathochromic shift values derived for CH<sub>2</sub>OO from the Sheps *et al.* (0.83/0.86 eV) and Ting *et al.* (0.69/0.73 eV), respectively.

#### **Conclusions**

In this manuscript, we have reported a systematic simulation of the electronic absorption spectra of CH<sub>2</sub>OO and CH<sub>3</sub>CHOO using a variety of excited-state quantum chemical methods with the view to develop an effective yet inexpensive way of computing the electronic absorption spectra of larger CIs. We have shown that the CASPT2 method with a moderate active space performs well for both CH<sub>2</sub>OO and CH<sub>3</sub>CHOO and is a good candidate for extension to CIs of greater molecular complexity, such as methacrolein oxide and methyl vinyl ketone oxide (both derived from isoprene ozonolysis), β-pinene oxide and CIs derived from the ozonolysis of endocyclic alkenes such as cyclopenta(di)ene and  $\alpha$ -pinene. As mentioned above, the ozonolysis of such large alkenes is likely to form CIs with extended  $\pi$ -conjugation, thereby shifting their electronic absorption maxima to within the peak of the tropospherically relevant solar spectral window. Additionally, two functionals of TDDFT (CAM-B3LYP and ωB97XD) were used to simulate the absorption profile of CH<sub>2</sub>OO and CH<sub>3</sub>CHOO. In both cases TDDFT overestimates the peak of the absorption profiles but the computation of the spectra using this method is considerably less expensive than multi-reference methods and some other single reference methods. A bathochromic shift value for each functional was derived for CH<sub>2</sub>OO in order to match with the experimentally measured electronic absorption spectrum. The same shift values were then

applied to the returned raw TDDFT spectrum of CH<sub>3</sub>CHOO and the agreement with the experimentally measured spectrum was remarkable.

The derivation of such bathochromic TDDFT shift values is important since a variety of CIs may be formed from the ozonolysis of a myriad of complex alkenes. Given the complicated electronic structure of CIs a shift value for a computationally inexpensive method is required in order to extend to CIs of greater molecular complexity.

We note however that the nuclear ensemble method has some shortcomings, as described in detail elsewhere. In short, it is unable to capture vibrational structure and any band asymmetry of the spectral profile. The artificial broadening of stick spectra from each Wigner geometry is largely arbitrarily defined. Lifetime broadening, for example, is uncaptured in the present method but would be a much more accurate way in defining the broadening factor  $\delta$  in equation 5. Trajectories could in principle be initiated at each Wigner geometry for short-propagation times in order to define a better value for  $\delta$ . Given these shortcomings, our presently simulated spectra are none-the-less informative as they are able to reproduce the peak maxima and photoabsorption cross sections reasonably well, which may then be used to extend to CIs of increasing molecular complexity with experimentally unknown UV absorption spectrum and thus guiding experimentalists towards their most likely probe wavelength regions.

It is also noteworthy that the choice of method for optimizing the ground state structure and computing the normal mode wavenumbers are also important factors, since the Wigner distribution of geometries is based on these. Our choice of B2PLYP-D3 for the optimization of the ground state geometry and normal mode calculations is motivated by previous studies that have shown this function to perform well when obtaining the ground state geometry and normal modes of Criegee intermediates. 47,48 Benchmark computations of the optimized parameters and

normal mode wavenumbers, using B2PLYP-D3, B3LYP and MP2, are given in tables S4 and S5 of the supporting information. In both cases only modest differences are observed; we therefore we do not expect significant differences in the spectral profiles calculated at a given level-of-theory, but when based on the ground state minimum energy geometry obtained by B2PLYP-D3, B3LYP or MP2.

In future studies we aim to extend the current methodology for computing the electronic absorption spectrum of more complex CIs. CASPT2 with a modest active space is adequate for the medium sized CIs and is likely to be in good agreement with the 'true' electronic absorption spectrum. For more complex CIs, TDDFT can be used effectively with the appropriate shift value.

Modelling the electronic absorption spectra of large CIs is paramount since most of these CIs do not have experimentally measured electronic absorption spectra. As a result, the returned results are expected to guide experiments in deciding the most appropriate wavelength regions to measure such larger CIs. Additionally, computing the electronic absorption spectra using this simple and versatile method will provide crucial information on whether photoexcitation, and subsequent excited state chemistry contributes to the removal process of larger CIs.

In future, we plan to implement our methodology into our SArCASM package<sup>66</sup> in an automated way. The user would need to specify the number of points, the level-of-theory (and active space if required) and SArCASM calls the necessary quantum chemical programs to calculate the energies, transition dipole moments and/or oscillator strengths and outputs the absorption profile. This interface allows for computation of the electronic absorption spectrum in a simple and accurate manner.

Acknowledgements

The work reported in this manuscript was funded by the National Science Foundation, under

grant agreement no. CHE-2003422. TNVK and JCM also acknowledges the Ray P. Authement

College of Sciences and the Department of Chemistry at UL Lafayette for financial support in

the form of startup funds and an undergraduate research assistantship, respectively.

The authors declare no conflicts of interest

**ORCID ID:** 

Barbara Marchetti: 0000-0002-0661-9029

Mushir Thodika: 0000-0002-6837-9710

Tolga N. V. Karsili: 0000-0002-0583-3824

**Supporting information:** 

Unshifted raw electronic absorption profiles of syn- and anti- CH<sub>3</sub>CHOO using TDDFT;

Unshifted raw electronic absorption profiles of CH<sub>2</sub>OO using various TDDFT functionals;

Vertical excitation energies, oscillator strengths and dominant electron promotions of CH<sub>2</sub>OO at

selected Wigner geometries; Cartesian coordinates of the ground state minimum energy

geometries; A comparison of the optimized parameters of CH<sub>2</sub>OO calculated at the B2PLYP-D3,

B3LYP and MP2 levels of theory; A comparison of the normal mode wavenumbers of CH2OO

calculated at the B2PLYP-D3, B3LYP and MP2 levels of theory.

### References

- (1) Donahue, N. M.; Drozd, G. T.; Epstein, S. A.; Presto, A. A.; Kroll, J. H. Adventures in Ozoneland: Down the Rabbit-Hole. *Phys. Chem. Chem. Phys.* **2011**, *13* (23), 10848–10857.
- (2) Khan, M. A. H.; Percival, C. J.; Caravan, R. L.; Taatjes, C. A.; Shallcross, D. E. Criegee Intermediates and Their Impacts on the Troposphere. *Environ. Sci. Process. Impacts* **2018**, 20 (3), 437–453.
- (3) Taatjes, C. A. Criegee Intermediates: What Direct Production and Detection Can Teach
  Us About Reactions of Carbonyl Oxides. *Annu. Rev. Phys. Chem.* **2017**, *68* (1), 183–207.
- (4) Lester, M. I.; Klippenstein, S. J. Unimolecular Decay of Criegee Intermediates to OH Radical Products: Prompt and Thermal Decay Processes. *Acc. Chem. Res.* **2018**, *51* (4), 978–985.
- (5) Ting, W. L.; Chen, Y. H.; Chao, W.; Smith, M. C.; Lin, J. J. M. The UV Absorption Spectrum of the Simplest Criegee Intermediate CH 2OO. *Phys. Chem. Chem. Phys.* **2014**, *16* (22), 10438–10443.
- (6) Smith, M. C.; Ting, W. L.; Chang, C. H.; Takahashi, K.; Boering, K. A.; Lin, J. J. M. UV Absorption Spectrum of the C2 Criegee Intermediate CH3CHOO. *J. Chem. Phys.* **2014**, *141* (7), 074302.
- (7) Lee, Y.-P. Perspective: Spectroscopy and Kinetics of Small Gaseous Criegee Intermediates. *J. Chem. Phys.* **2015**, *143* (2), 20901.
- (8) Song, M.; Zhang, C.; Wu, H.; Mu, J.; Ma, Z.; Liu, P.; Liu, J.; Zhang, Y.; Chen, C.; Fu, Y.; et al. The Influence of UV-Light Irradiation and Stable Criegee Intermediate Scavengers

- on Secondary Organic Aerosol Formation from Isoprene Ozonolysis. *Atmos. Environ.* **2018**, *191* (August), 116–125.
- (9) Chang, Y. P.; Li, Y. L.; Liu, M. L.; Ou, T. C.; Lin, J. J. M. Absolute Infrared Absorption Cross Section of the Simplest Criegee Intermediate Near 1285.7 Cm-1. *J. Phys. Chem. A* 2018, 122 (45), 8874–8881.
- (10) Ting, W. L.; Chen, Y. H.; Chao, W.; Smith, M. C.; Lin, J. J. M. The UV Absorption Spectrum of the Simplest Criegee Intermediate CH 200. *Phys. Chem. Chem. Phys.* **2014**, *16* (22), 10438–10443.
- (11) Ting, A. W.-L.; Lin, J. J.-M. UV Spectrum of the Simplest Deuterated Criegee Intermediate CD2OO. *J. Chinese Chem. Soc.* **2017**, *64* (4), 360–368.
- Chang, Y.-P.; Chang, C.-H.; Takahashi, K.; Lin, J. J.-M. Absolute UV Absorption Cross Sections of Dimethyl Substituted Criegee Intermediate (CH3)2COO. *Chem. Phys. Lett.* 2016, 653, 155–160.
- (13) Sheps, L.; Scully, A. M.; Au, K. UV Absorption Probing of the Conformer-Dependent Reactivity of a Criegee Intermediate CH3CHOO. *Phys. Chem. Chem. Phys.* **2014**, *16* (48), 26701–26706.
- (14) Sheps, L. Absolute Ultraviolet Absorption Spectrum of a Criegee Intermediate CH 2OO.J. Phys. Chem. Lett. 2013, 4 (24), 4201–4205.
- (15) Sršeň; Hollas, D.; Slavíček, P. UV Absorption of Criegee Intermediates: Quantitative
   Cross Sections from High-Level: Ab Initio Theory. *Phys. Chem. Chem. Phys.* 2018, 20
   (9), 6421–6430.
- (16) Dawes, R.; Jiang, B.; Guo, H. UV Absorption Spectrum and Photodissociation Channels

- of the Simplest Criegee Intermediate (CH2OO). J. Am. Chem. Soc. 2015, 137 (1), 50-53.
- (17) Aplincourt, P.; Henon, E.; Bohr, F.; Ruiz-López, M. F. Theoretical Study of Photochemical Processes Involving Singlet Excited States of Formaldehyde Carbonyl Oxide in the Atmosphere. *Chem. Phys.* 2002, 285 (2–3), 221–231.
- (18) Foreman, E. S.; Kapnas, K. M.; Jou, Y. T.; Kalinowski, J.; Feng, D.; Gerber, R. B.; Murray, C. High Resolution Absolute Absorption Cross Sections of the B1A'-X1A' Transition of the CH2OO Biradical. *Phys. Chem. Chem. Phys.* 2015, *17* (48), 32539–32546.
- (19) Liu, F.; Beames, J. M.; Green, A. M.; Lester, M. I. UV Spectroscopic Characterization of Dimethyl- and Ethyl-Substituted Carbonyl Oxides. *J. Phys. Chem. A* 2014, 118 (12), 2298–2306.
- (20) Beames, J. M.; Liu, F.; Lu, L.; Lester, M. I. UV Spectroscopic Characterization of an Alkyl Substituted Criegee Intermediate CH3CHOO. *J. Chem. Phys.* **2013**, *138* (24), 244307.
- (21) Kalinowski, J.; Foreman, E. S.; Kapnas, K. M.; Murray, C.; Räsänen, M.; Benny Gerber,
  R. Dynamics and Spectroscopy of CH2OO Excited Electronic States. *Phys. Chem. Chem. Phys.* 2016, *18* (16), 10941–10946.
- (22) Beames, J. M.; Liu, F.; Lu, L.; Lester, M. I. Ultraviolet Spectrum and Photochemistry of the Simplest Criegee Intermediate CH2OO. *J. Am. Chem. Soc.* **2012**, *134* (49), 20045–20048.
- (23) Yin, C.; Takahashi, K. How Big Is the Substituent Dependence of the Solar Photolysis Rate of Criegee Intermediates? *Phys. Chem. Chem. Phys.* **2018**, *20* (23), 16247–16255.

- (24) Li, H.; Fang, Y.; Kidwell, N. M.; Beames, J. M.; Lester, M. I. UV Photodissociation Dynamics of the CH3CHOO Criegee Intermediate: Action Spectroscopy and Velocity Map Imaging of O-Atom Products. *J. Phys. Chem. A* 2015, *119* (30), 8328–8337.
- (25) Lehman, J. H.; Li, H.; Beames, J. M.; Lester, M. I. Communication: Ultraviolet Photodissociation Dynamics of the Simplest Criegee Intermediate CH2OO. *J. Chem. Phys.* **2013**, *139* (14), 141103.
- (26) Vansco, M. F.; Li, H.; Lester, M. I. Prompt Release of O 1D Products upon UV Excitation of CH2OO Criegee Intermediates. *J. Chem. Phys.* **2017**, *147* (1), 13907.
- (27) Samanta, K.; Beames, J. M.; Lester, M. I.; Subotnik, J. E. Quantum Dynamical Investigation of the Simplest Criegee Intermediate CH2OO and Its O–O Photodissociation Channels. J. Chem. Phys. 2014, 141 (13), 134303.
- (28) Sheps, L.; Scully, A. M.; Au, K. UV Absorption Probing of the Conformer-Dependent Reactivity of a Criegee Intermediate CH3CHOO. *Phys. Chem. Chem. Phys.* **2014**, *16* (48), 26701–26706.
- (29) Taatjes, C. A.; Welz, O.; Eskola, A. J.; Savee, J. D.; Osborn, D. L.; Lee, E. P. F.; Dyke, J. M.; Mok, D. W. K.; Shallcross, D. E.; Percival, C. J. Direct Measurement of Criegee Intermediate (CH2OO) Reactions with Acetone, Acetaldehyde, and Hexafluoroacetone.
  Phys. Chem. Chem. Phys. 2012, 14 (30), 10391–10400.
- (30) Welz, O.; Savee, J. D.; Osborn, D. L.; Vasu, S. S.; Percival, C. J.; Shallcross, D. E.;
  Taatjes, C. A. Direct Kinetic Measurements of Criegee Intermediate (CH2OO) Formed by
  Reaction of CH2I with O2. *Science* (80-. ). 2012, 335 (6065), 204–207.
- (31) Taatjes, C. A.; Welz, O.; Eskola, A. J.; Savee, J. D.; Scheer, A. M.; Shallcross, D. E.;

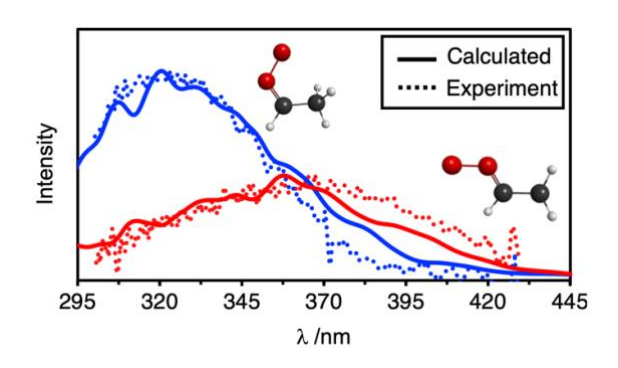
- Rotavera, B.; Lee, E. P. F.; Dyke, J. M.; Mok, D. K. W.; et al. Direct Measurements of Conformer-Dependent Reactivity of the Criegee Intermediate CH3CHOO. *Science* (80-.). **2013**, *340* (6129), 177–180.
- (32) Anglada, J. M.; González, J.; Torrent-Sucarrat, M. Effects of the Substituents on the Reactivity of Carbonyl Oxides. A Theoretical Study on the Reaction of Substituted Carbonyl Oxides with Water. *Phys. Chem. Chem. Phys.* **2011**, *13* (28), 13034–13045.
- (33) Trabelsi, T.; Kumar, M.; Francisco, J. S. Substituent Effects on the Spectroscopic Properties of Criegee Intermediates. *J. Chem. Phys.* **2017**, *147* (16), 164303.
- (34) Jr-Min Lin, J.; Chao, W. Structure-Dependent Reactivity of Criegee Intermediates Studied with Spectroscopic Methods. *Chem. Soc. Rev.* **2017**, *46* (24), 7483–7497.
- (35) Vansco, M. F.; Marchetti, B.; Lester, M. I. Electronic Spectroscopy of Methyl Vinyl Ketone Oxide: A Four-Carbon Unsaturated Criegee Intermediate from Isoprene Ozonolysis. J. Chem. Phys. 2018, 149 (24), 244309.
- (36) Vansco, M. F.; Marchetti, B.; Trongsiriwat, N.; Bhagde, T.; Wang, G.; Walsh, P. J.; Klippenstein, S. J.; Lester, M. I. Synthesis, Electronic Spectroscopy, and Photochemistry of Methacrolein Oxide: A Four-Carbon Unsaturated Criegee Intermediate from Isoprene Ozonolysis. *J. Am. Chem. Soc.* 2019, *141* (38), 15058–15069.
- (37) Crespo-Otero, R.; Barbatti, M. Spectrum Simulation and Decomposition with Nuclear Ensemble: Formal Derivation and Application to Benzene, Furan and 2-Phenylfuran. *Theor. Chem. Acc.* **2012**, *131* (6), 1–14.
- (38) McGillen, M. R.; Curchod, B. F. E.; Chhantyal-Pun, R.; Beames, J. M.; Watson, N.; Khan, M. A. H.; McMahon, L.; Shallcross, D. E.; Orr-Ewing, A. J. Criegee Intermediate-

- Alcohol Reactions, A Potential Source of Functionalized Hydroperoxides in the Atmosphere. *ACS Earth Sp. Chem.* **2017**, *I* (10), 664–672.
- (39) Yu, X.; Hou, H.; Wang, B. Atmospheric Chemistry of Perfluoro-3-Methyl-2-Butanone [CF3C(O)CF(CF3)2]: Photodissociation and Reaction with OH Radicals. *J. Phys. Chem. A* **2018**, *122* (45), 8840–8848.
- (40) Francés-Monerris, A.; Carmona-García, J.; Acuña, A. U.; Dávalos, J. Z.; Cuevas, C. A.; Kinnison, D. E.; Francisco, J. S.; Saiz-Lopez, A.; Roca-Sanjuán, D. Photodissociation Mechanisms of Major Mercury(II) Species in the Atmospheric Chemical Cycle of Mercury. *Angew. Chemie Int. Ed.* 2020, 59 (19), 7605–7610.
- (41) Prlj, A.; Ibele, L. M.; Marsili, E.; Curchod, B. F. E. On the Theoretical Determination of Photolysis Properties for Atmospheric Volatile Organic Compounds. *J. Phys. Chem. Lett.* 2020, 11 (14), 5418–5425.
- (42) Röder, A.; de Oliveira, N.; Grollau, F.; Mestdagh, J.-M.; Gaveau, M.-A.; Briant, M. Vacuum-Ultraviolet Absorption Spectrum of 3-Methoxyacrylonitrile. *J. Phys. Chem. A* **2020**, *124* (45), 9470–9477.
- (43) Rodrigues, G. P.; Ventura, E.; Andrade do Monte, S.; Barbatti, M. UV-Photoexcitation and Ultrafast Dynamics of HCFC-132b (CF2ClCH2Cl). *J. Comput. Chem.* **2016**, *37* (7), 675–683.
- (44) Saiz-Lopez, A.; Sitkiewicz, S. P.; Roca-Sanjuán, D.; Oliva-Enrich, J. M.; Dávalos, J. Z.; Notario, R.; Jiskra, M.; Xu, Y.; Wang, F.; Thackray, C. P.; et al. Photoreduction of Gaseous Oxidized Mercury Changes Global Atmospheric Mercury Speciation, Transport and Deposition. *Nat. Commun.* 2018, 9 (1), 4796.

- (45) Grimme, S. Semiempirical Hybrid Density Functional with Perturbative Second-Order Correlation. *J. Chem. Phys.* **2006**, *124* (3), 34108.
- (46) Dunning, T. H. Gaussian Basis Sets for Use in Correlated Molecular Calculations. I. The Atoms Boron through Neon and Hydrogen. *J. Chem. Phys.* **1989**, *90* (2), 1007–1023.
- (47) Barber, V. P.; Pandit, S.; Esposito, V. J.; McCoy, A. B.; Lester, M. I. CH Stretch Activation of CH3CHOO: Deep Tunneling to Hydroxyl Radical Products. *J. Phys. Chem. A* **2019**, *123* (13), 2559–2569.
- (48) Barber, V. P.; Pandit, S.; Green, A. M.; Trongsiriwat, N.; Walsh, P. J.; Klippenstein, S. J.; Lester, M. I. Four-Carbon Criegee Intermediate from Isoprene Ozonolysis: Methyl Vinyl Ketone Oxide Synthesis, Infrared Spectrum, and OH Production. *J. Am. Chem. Soc.* 2018, 140 (34), 10866–10880.
- (49) Barbatti, M.; Ruckenbauer, M.; Plasser, F.; Pittner, J.; Granucci, G.; Persico, M.; Lischka, H. Newton-X: A Surface-Hopping Program for Nonadiabatic Molecular Dynamics. *Wiley Interdiscip. Rev. Comput. Mol. Sci.* **2013**, *4* (1), 26–33.
- (50) Barbatti, M.; Sen, K. Effects of Different Initial Condition Samplings on Photodynamics and Spectrum of Pyrrole. *Int. J. Quantum Chem.* **2015**, *116* (10), 762–771.
- (51) Roos, B. O.; Linse, P.; Siegbahn, P. E. M.; Blomberg, M. R. A. A Simple Method for the Evaluation of the Second-Order-Perturbation Energy from External Double-Excitations with a CASSCF Reference Wavefunction. *Chem. Phys.* **1982**, *66* (1), 197–207.
- (52) Andersson, K.; Malmqvist, P. A.; Roos, B. O.; Sadlej, A. J.; Wolinski, K. Second-Order Perturbation Theory with a CASSCF Reference Function. *J. Phys. Chem.* **1990**, *94* (14), 5483–5488.

- (53) Andersson, K.; Malmqvist, P.; Roos, B. O. Second-order Perturbation Theory with a
   Complete Active Space Self-consistent Field Reference Function. *J. Chem. Phys.* 1992, 96
   (2), 1218–1226.
- (54) Shiozaki, T.; Werner, H.-J. Communication: Second-Order Multireference Perturbation Theory with Explicit Correlation: CASPT2-F12. *J. Chem. Phys.* **2010**, *133* (14), 141103.
- (55) Knowles, P. J.; Werner, H.-J. An Efficient Method for the Evaluation of Coupling Coefficients in Configuration Interaction Calculations. *Chem. Phys. Lett.* **1988**, *145* (6), 514–522.
- (56) Werner, H.; Knowles, P. J. An Efficient Internally Contracted Multiconfiguration— Reference Configuration Interaction Method. *J. Chem. Phys.* **1988**, *89* (9), 5803–5814.
- (57) Chai, J.-D.; Head-Gordon, M. Long-Range Corrected Hybrid Density Functionals with Damped Atom-Atom Dispersion Corrections. *Phys. Chem. Chem. Phys.* **2008**, *10* (44), 6615–6620.
- (58) Yanai, T.; Tew, D. P.; Handy, N. C. A New Hybrid Exchange–Correlation Functional Using the Coulomb-Attenuating Method (CAM-B3LYP). *Chem. Phys. Lett.* **2004**, *393* (1), 51–57.
- (59) Hehre, W. J.; Ditchfield, R.; Stewart, R. F.; Pople, J. A. Self-Consistent Molecular Orbital Methods. IV. Use of Gaussian Expansions of Slater-Type Orbitals. Extension to Second-Row Molecules. J. Chem. Phys. 1970, 52 (5), 2769–2773.
- (60) Hehre, W. J.; Stewart, R. F.; Pople, J. A. Self-Consistent Molecular-Orbital Methods. I.
  Use of Gaussian Expansions of Slater-Type Atomic Orbitals. *J. Chem. Phys.* 1969, 51 (6), 2657–2664.

- (61) Barbatti, M.; Granucci, G.; Persico, M.; Ruckenbauer, M.; Vazdar, M.; Eckert-Maksić, M.; Lischka, H. The On-the-Fly Surface-Hopping Program System Newton-X: Application to Ab Initio Simulation of the Nonadiabatic Photodynamics of Benchmark Systems. *J. Photochem. Photobiol. A Chem.* 2007, 190 (2), 228–240.
- (62) , M. J. Frisch, G. W. Trucks, H. B. Schlegel, G. E. Scuseria, M. A. Robb, J. R.
  Cheeseman, G. Scalmani, V. Barone, G. A. Petersson, H. Nakatsuji, X. Li, M. Caricato,
  A. V. Marenich, J. Bloino, B. G. Janesko, R. Gomperts, B. Mennucci, H. P. Hratchian, J.
  V, and D. J. F. Gaussian 16, Revision C.01. *Gaussian Inc. Wallingford CT* 2016.
- (63) Werner, H.-J.; Knowles, P. J.; Knizia, G.; Manby, F. R.; Schütz, M.; Celani, P.; Györffy, W.; Kats, D.; Korona, T.; Lindh, R.; et al. MOLPRO, Version 2018.1, a Package of Ab Initio Programs. 2018.
- (64) Werner, H.-J.; Knowles, P. J.; Knizia, G.; Manby, F. R.; Schütz, M. Molpro: A General-Purpose Quantum Chemistry Program Package. *WIREs Comput. Mol. Sci.* **2012**, *2* (2), 242–253.
- (65) Crespo-Otero, R.; Barbatti, M. Recent Advances and Perspectives on Nonadiabatic Mixed Quantum–Classical Dynamics. *Chem. Rev.* **2018**, *118* (15), 7026–7068.
- (66) Karsili, T. N. V.; Thodika, M.; Nguyen, L.; Matsika, S. The Origin of Fluorescence in DNA Thio-Analogues. *Chem. Phys.* **2018**, No. August, 1–7.



For Table of Contents Only